Targeted positron emission tomography imaging of CXCR4 expression in patients with acute myeloid leukemia

Peter Herhaus,[1] Stefan Habringer,[1,2,#] Kathrin Philipp-Abbrederis,[1] Tibor Vag,[3] Carlos Gerngross,[3] Margret Schottelius,[4] Julia Slotta-Huspenina,[5] Katja Steiger,[5] Torben Altmann,[6] Tanja Weißer,[1] Sabine Steidle,[1] Markus Schick,[1] Laura Jacobs,[3] Jolanta Slawska,[3] Catharina Müller-Thomas,[1] Mareike Verbeek,[1] Marion Subklewe,[2,6] Christian Peschel,[1,2] Hans-Jürgen Wester,[5] Markus Schwaiger,[2,3] Katharina Götze,[1,2] and Ulrich Keller[1,2]

[1]III Medical Department, Technische Universität München; [2]German Cancer Consortium (DKTK), German Cancer Research Center (DKFZ), Heidelberg; [3]Nuclear Medicine Department, Technische Universität München; [4]Pharmaceutical Radiochemistry, Technische Universität München; [5]Department of Pathology, Technische Universität München; and [6]III Medical Department, Ludwig-Maximilians-Universität, Munich, Germany

[#]PH and SH contributed equally to this work.

Haematologica 2016
Volume 101(8):932-940

Correspondence:

ulrich.keller@tum.de

Received: January 18, 2016.

Accepted: May 4, 2016.

Pre-published: May 12, 2016.

doi:10.3324/haematol.2016.142976

Check the online version for the most updated information on this article, online supplements, and information on authorship & disclosures: www.haematologica.org/content/101/8/932

ABSTRACT

Acute myeloid leukemia originates from leukemia-initiating cells that reside in the protective bone marrow niche. CXCR4/CXCL12 interaction is crucially involved in recruitment and retention of leukemia-initiating cells within this niche. Various drugs targeting this pathway have entered clinical trials. To evaluate CXCR4 imaging in acute myeloid leukemia, we first tested CXCR4 expression in patient-derived primary blasts. Flow cytometry revealed that high blast counts in patients with acute myeloid leukemia correlate with high CXCR4 expression. The wide range of CXCR4 surface expression in patients was reflected in cell lines of acute myeloid leukemia. Next, we evaluated the CXCR4-specific peptide Pentixafor by positron emission tomography imaging in mice harboring CXCR4 positive and CXCR4 negative leukemia xenografts, and in 10 patients with active disease. [^{68}Ga]Pentixafor-positron emission tomography showed specific measurable disease in murine CXCR4 positive xenografts, but not when CXCR4 was knocked out with CRISPR/Cas9 gene editing. Five of 10 patients showed tracer uptake correlating well with leukemia infiltration assessed by magnetic resonance imaging. The mean maximal standard uptake value was significantly higher in visually CXCR4 positive patients compared to CXCR4 negative patients. In summary, *in vivo* molecular CXCR4 imaging by means of positron emission tomography is feasible in acute myeloid leukemia. These data provide a framework for future diagnostic and theranostic approaches targeting the CXCR4/CXCL12-defined leukemia-initiating cell niche.

Introduction

Acute myeloid leukemia (AML) is an aggressive hematologic neoplasm originating from a myeloid hematopoietic stem/precursor cell (HSPC). AML is rapidly fatal if untreated. Although rates of complete remission after initial induction chemotherapy approach 70%, many patients relapse. Prognosis remains particularly dismal for those patients with adverse prognostic disease features (i.e. poor risk cytogenetics and/or poor risk molecular genetics), as well as for elderly patients unable to undergo intensive therapy, highlighting the clinical need for effective novel therapeutic strategies.[1-3]

Acute myeloid leukemia relapses are thought to arise from quiescent leukemia-

initiating cells (LIC) harbored by the specialized bone marrow (BM) microenvironment, termed the stem cell niche. Several pre-clinical studies have shown that LICs are resistant to conventional chemotherapy as well as targeted therapy, and are selectively protected by interaction with the stem cell niche. Cross-talk between LICs and niche cells has also been demonstrated to be important for disease maintenance and progression.[4-6] Thus, targeting the BM niche is an emerging and attractive therapeutic concept in AML.

CXC-motif chemokine receptor 4 (CXCR4) functions together with its sole known chemokine ligand CXCL12 (also named Stromal cell-derived factor-1, SDF-1) as a master regulator of leukocyte migration and homing, and of HSPC retention in BM niches.[7-11] CXCR4 is physiologically expressed on myeloid and lymphoid cells as well as on subtypes of epithelial cells. The activation of the CXCR4/CXCL12 pathway has been identified in several hematologic and solid malignancies.[12] In this context, the CXCR4/CXCL12 axis is a key regulator of proliferation, chemotaxis to organs that secrete CXCL12, and aberrant angiogenesis, all of which are pivotal mechanisms of tumor progression and metastasis.[13] The interaction between CXCR4 on malignant cells and secreted CXCL12 from the microenvironment is a fundamental component of the crosstalk between LIC and their niche.[14] The CXCR4/CXCL12 axis is essential for both normal and leukemic HSPC migration *in vivo*.[15,16] In NOD/SCID mice, homing and subsequent engraftment of normal human or AML HSPC are dependent on the expression of cell surface CXCR4, and CXCL12 produced within the murine BM niche.[9,14]

As shown for several other cancers, CXCR4 expression negatively impacts prognosis in AML.[17] Recent data in acute lymphoblastic leukemia (ALL) further substantiate the crucial role of this interaction in acute leukemia.[18,19] Therefore, targeting CXCR4 and the CXCR4/CXCL12-defined LIC niche is an obvious and highly promising approach for long-term cure of hematopoietic stem cell malignancies, and CXCR4 is clearly a druggable target. Consequently, several novel therapies involving antibodies or small molecule drugs directed against CXCR4 or CXCL12 are currently being evaluated in clinical trials, with encouraging results.[20-22]

Our previous work identified the high affinity/specificity CXCR4-binding peptide Pentixafor as a suitable tracer for molecular *in vivo* CXCR4 positron emission tomography (PET) imaging in lymphoid malignancies.[23,24] Beyond imaging, however, and in particular in systemic malignancies like lymphoma and leukemia, the real impact of such a peptide would be its therapeutic application. Pentixafor labeled to therapeutic radionuclides is feasible and has already been applied in individual patients with multiple myeloma,[25] and a phase I/II clinical trial is currently under investigation (*EudraCT: 2015-001817-28*). The data presented here identify CXCR4 as a suitable target for imaging in AML, implying the potential for CXCR4-directed peptide-receptor radiotherapy (PRRT) in acute leukemia.

Methods

Patients

Samples from 67 unselected patients with active myeloid disease (myelodysplastic syndrome (MDS), *de novo* AML or secondary AML (sAML) were investigated for CXCR4 surface expression by flow cytometry.

Ten patients with active myeloid disease underwent PET imaging for CXCR4. Five patients with non-hematologic malignancies examined through different analytical approaches served as controls. As previously reported for other [^{68}Ga]-labeled peptides,[26] [^{68}Ga]Pentixafor was administered under the conditions of pharmaceutical law (The German Medicinal Products Act, AMG, Section 13, 2b) according to the German law and in accordance with the regulatory agencies responsible (Regierung von Oberbayern). All patients gave written informed consent prior to the investigation. The Ethics Committee of the Technische Universität München approved data analysis. Detailed information on patients' characteristics are provided in the *Online Supplementary Appendix*.

Cell lines

The following human AML cell lines were used: Molm-13, MV4-11, NOMO-1, NB4, KG1a, OCI-AML2, OCI-AML3, Mono-Mac-1, Mono-Mac-6, OCI-AML5, GF-D8. The human Burkitt lymphoma line Daudi served as a positive control for CXCR4 expression. For details see the *Online Supplementary Appendix*.

RNA isolation and real-time PCR

Assessment of CXCR4 mRNA of AML cell lines was performed as described in the *Online Supplementary Appendix*.

CRISPR-Cas9 mediated knock-out of CXCR4

OCI-AML3 cells were stably transduced with lentiCRISPRv2 (Addgene plasmid #52961), coding for Cas9 and a CXCR4-specific sgRNA. Indel formation was assessed as described previously.[27] Additional information is provided in the *Online Supplementary Appendix*.

Migration assay

Cell migration towards CXCL12 (R&D Systems, Minneapolis, MN, USA) was performed in transwell plates with 5 μm pore size (Corning Inc., Corning, NY, USA) and was quantified with CountBright beads (Thermo Fisher, Waltham, MA, USA). For details see the *Online Supplementary Appendix*.

Mice and tumor xenograft experiments

Animal studies were performed in agreement with the Guide for Care and Use of Laboratory Animals published by the US National Institutes of Health (NIH Publication n. 85-23, revised 1996), in compliance with the German law on the protection of animals, and with the approval of the regional authorities responsible (Regierung von Oberbayern). PET scans of xenotransplanted AML cell lines in SCID mice were performed as previously described[24] and are described briefly in the *Online Supplementary Appendix*.

Flow cytometry and immunohistochemistry

The following antibodies were used for flow cytometry: Beckman Coulter: CD45-ECD (clone J33), CD34-FITC (clone 581), CD117-PE (clone 104D2D1); BD Biosciences (Franklin Lakes, NJ, USA): CXCR4-PE (clone 12G5), PE mouse IgG2a (Clone G155-178); for immunohistochemistry: ab12482 (clone UMB-2, abcam, Cambridge, UK), CD34 (QBEnd/10, Cell Marque), CD117 (c-kit, Dako), CD43 (Novocastra). Further details are provided in the *Online Supplementary Appendix*.

PET/MR and PET/CT imaging studies in patients and animals

[^{68}Ga]Pentixafor was synthesized and PET/MRI analysis was performed as previously described.[28-33] Detailed descriptions of

imaging protocols are provided in the *Online Supplementary Appendix.*

Statistical analysis

All statistical tests were performed using GraphPad Prism (GraphPad Software, La Jolla, CA, USA). $P<0.05$ was considered statistically significant. Quantitative values were expressed as mean±standard deviation (SD) or standard error of the mean (SEM) as indicated. Additional information is given in the *Online Supplementary Appendix.*

Results

CXCR4 is highly expressed on leukemic blasts in a subset of AML patients

To address CXCR4 abundance in myeloid malignancies, we first assessed CXCR4 expression in an unselected cohort of 67 consecutive patients with active disease (AML, MDS) by flow cytometry of bone marrow (BM) and/or peripheral blood (PB). For details of patients' characteristics see *Online Supplementary Table S1*. Myeloid blasts were gated as $CD45^{dim}$ cells, and CD117 was used as a marker for myeloid blasts (gating strategy depicted in *Online Supplementary Figure S1A*). Lymphocytes with known CXCR4 positivity served as an intraindividual control (*Online Supplementary Figure S1B*). These analyses revealed a wide range of surface CXCR4 expression on myeloid blasts, from virtually absent expression to high levels in a distinct subset of AML patients. Representative flow cytometry data from AML patients are shown in Figure 1A. Quantification of CXCR4 surface expression showed significantly higher CXCR4 expression in patients with a blast percentage exceeding 30%. There was a trend towards higher CXCR4 expression in blasts derived from AML samples compared to MDS samples (Figure 1B and C). No significant correlation between high CXCR4 expression on blasts and disease stage (first diagnosis *vs.* refractory/relapsed disease), *de novo vs.* sAML, age (<65 *vs.* ≥65 years), prognostic risk group according to the modified ELN classification[34] or existing genetic aberrations was found (*Online Supplementary Figure S2A-F*). No significantly different CXCR4 surface expression in paired PB and BM samples was observed (*Online Supplementary Figure S2G*).

[^{68}Ga]Pentixafor-PET enables in vivo CXCR4 imaging of AML xenografts

Since CXCR4 is an attractive target for novel therapeutic approaches directed against the leukemic microenvironment, we sought to evaluate the clinical applicability of the novel CXCR4-binding PET tracer Pentixafor labeled with a Gallium isotope (^{68}Ga), [^{68}Ga]Pentixafor, in myeloid malignancies. To select appropriate AML cell lines to model AML with detectable CXCR4 expression, transcript levels and surface expression of CXCR4 was evaluated in ten established AML cell lines. As expected from flow cytometry data in AML patients (Figure 1), CXCR4 expression in cell lines ranged from low (KG1a) to high (NOMO-1, OCI-AML3) (Figure 2A and B). CXCR4 surface expression assessed by flow cytometry correlated with transcript levels (Figure 2C and D). Of all cell lines analyzed, OCI-AML3 showed the highest expression and was, therefore, chosen as a cell line for modeling CXCR4-high AML in further imaging experiments.

To test if PET imaging of AML cells with [^{68}Ga]Pentixafor was feasible *in vivo*, we chose OCI-AML3 and NOMO-1 as $CXCR4^{high}$ and KG1a as $CXCR4^{low}$ cell line to generate subcutaneous xenograft mouse models. After tumor engraftment was apparent in all mice, [^{68}Ga]Pentixafor and PET imaging was performed. NOMO-1 and OCI-AML3 xenografts were clearly visible, whereas KG1a xenografts were not (Figure 3A), demonstrating that CXCR4-high AML cells can be visualized with [^{68}Ga]Pentixafor *in vivo*.

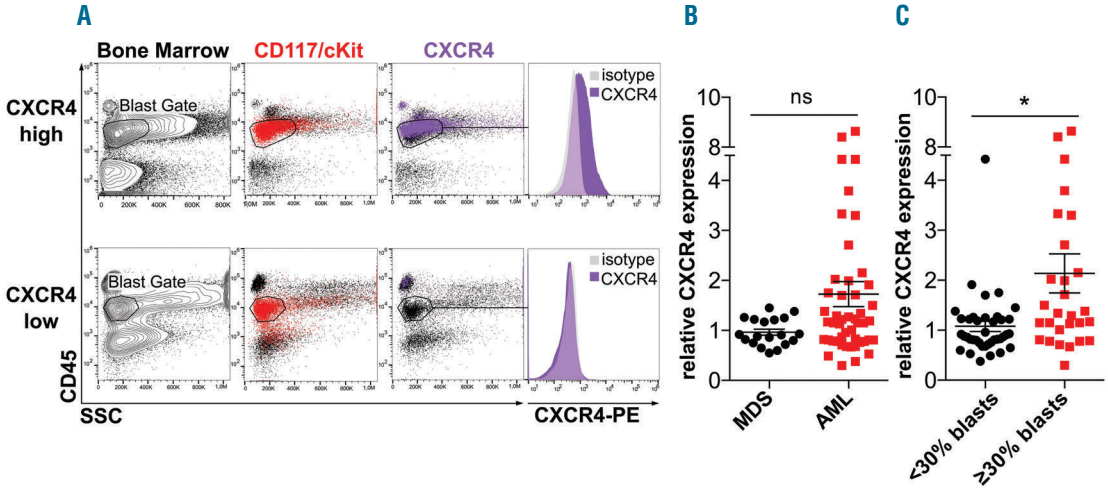

Figure 1. CXCR4 expression in patients with acute myeloid leukemia (AML) and myelodysplastic syndromes (MDS). (A) Flow cytometric evaluation of CXCR4 surface expression using an anti-CXCR4 antibody. Blasts were gated as $CD45^{low}$ cell population. Anti-CD117 antibody was used for back-gating. Representative data of CXCR4 positive (upper panels) and CXCR4 negative (lower panels) patients are shown. (B and C) Median fluorescence intensity of surface CXCR4 expression relative to isotype control (n=67 patients). Horizontal bars indicate the mean of all individual patient values±SEM; Student's *t*-test was used to compare mean relative blast CXCR4 expression. *Statistically significant differences between the groups. (B) MDS *versus* AML; $P=0.062$. (C) CXCR4 expression in patients with less than 30% blasts *versus* CXCR4 expression in patients with at least 30% blasts; $P=0.004$.

To further test the specificity of [^{68}Ga]Pentixafor binding to CXCR4, OCI-AML3 cells were selected for a CRISPR-Cas9 based stable knock-out of CXCR4 using a modified lentiCRISPRv2 to co-express *Streptococcus pyogenes* Cas9 and sgRNAs directed against human CXCR4.[35] This approach resulted in effective indel formation in the CXCR4 gene (*Online Supplementary Figure S3A*), reduction of CXCR4 surface expression (Figure 3B) and CXCL12-dependent migration (Figure 3C), while the growth kinetics remained unaffected *in vivo* (Figure 3D) and *in vitro* (*Online Supplementary Figure S3C*). For *in vivo* experiments, sg2 (sequence in *Online Supplementary Figure S3A*), targeting exon 2 of CXCR4, was chosen. OCI-AML3 stably transduced with lentiCRISPRv2-sg2 and non-targeting lentiCRISPRv2 as control were subcutaneously injected into SCID mice. [^{68}Ga]Pentixafor-PET imaging of these AML xenografts showed that OCI-AML3 control cells could be detected, and knock-out of CXCR4 in the same cell line abolished binding and PET positivity of AML xenografts. Binding of the imaging probe to mouse tissues was low, owing to the known specificity of [^{68}Ga]Pentixafor to human CXCR4 (Figure 3B and E).

Thus, *in vivo* PET imaging of AML xenografts with [^{68}Ga]Pentixafor is feasible and enables visualizing AML cells in a CXCR4-dependent manner.

CXCR4 directed PET/MR imaging in patients with myeloid malignancies

Our findings in the AML xenograft model (Figure 3), the specific binding characteristics of [^{68}Ga]Pentixafor to human CXCR4,[23,24] as well as the expression data generated in the flow cytometry patient cohort (Figure 1) encouraged us to test if CXCR4 imaging was also feasible in patients with myeloid malignancies. For this purpose, CXCR4-directed PET was combined with MR imaging, a method that is suitable for evaluating replacement of normal BM by malignant processes, including AML.[36]

Ten patients underwent [^{68}Ga]Pentixafor-PET imaging after signing informed consent. In 9 of the 10 patients, PET was combined with a whole body magnetic resonance (MR) imaging approach. In one patient, a PET/CT was conducted. One patient with extramedullary relapse and absence of BM infiltration as shown by biopsy received [^{68}Ga]Pentixafor-PET/MR and standard [^{18}F]FDG-PET/CT. Eight of 10 patients who underwent PET/MR imaging had BM involvement of AML, and one had an MDS-RAEB2. For details of patients' characteristics see *Online Supplementary Table S3*.

Four out of 9 patients with BM involvement were visually positive as assessed by [^{68}Ga]Pentixafor-PET. The PET positive areas correlated well with the expected signal

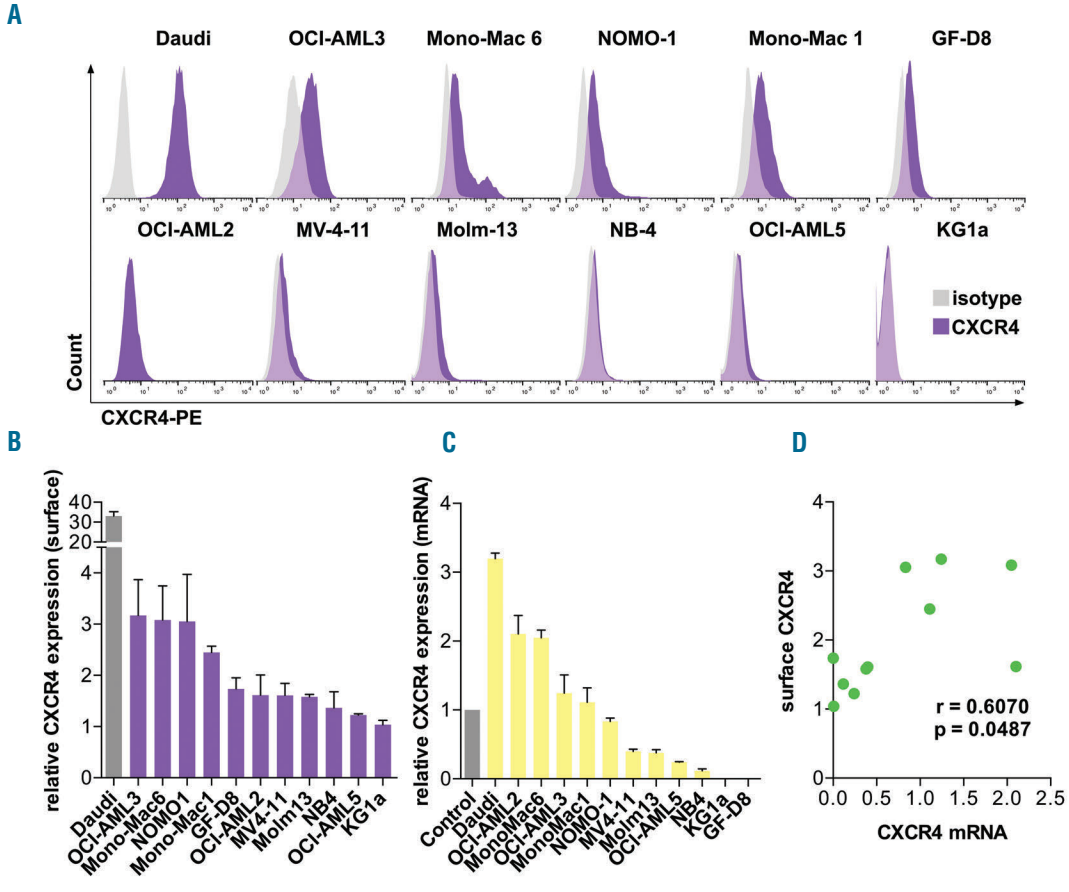

Figure 2. Surface CXCR4 expression of acute myeloid leukemia (AML) cell lines correlates with transcript levels. (A) Flow cytometric evaluation of CXCR4 surface expression of the indicated AML cell lines using an anti-CXCR4 antibody. An isotype control antibody was used as a control. (B) Mean fluorescence intensity of surface CXCR4 expression relative to isotype control. Three replicates for each cell line were used. (C) CXCR4 transcript levels measured by qRT-PCR. Mean relative expression±SEM is shown (n=3 independent experiments). ΔΔCt values relative to ubiquitin (Ub) were normalized to those of peripheral blood mononuclear cells (PBMC) of 3 healthy individuals. (D) Correlation analysis between relative CXCR4 transcript and relative CXCR4 surface expression levels.

alterations as determined by MR imaging (n=4, representative images shown in Figure 4A-F). Five of the 9 patients were visually graded as PET negative (representative images shown in Figure 4G-I). To clearly depict those differences between PET positive and negative AML and control patients, the vertebra are the best examples. Whereas all AML patients show decreased BM signal in the T1w MR sequences (Figure 4B, E, H), those BM areas only show elevated tracer uptake in the PET positive patients (Figure 4C and F). The tracer uptake within the infiltrated BM areas of the PET negative AML patient (Figure 4I) resembles those of the control patient without BM signal alterations in T1w MR sequences (Figure 4K and L). In order to allow for standardized evaluation of SUV, 5 anatomic locations with active hematopoiesis in adults were chosen for the quantification of the PET signal (Figure 4M). Compared to visually PET negative AML patients and patients with non-hematologic malignancies, the SUVmax of the five pre-defined areas of measurement was significantly higher in PET positive patients (Figure 4M). The calculated meanSUVmax was significantly higher in patients with PET positive AML compared to PET negative AML (Figure 4N). One of the 10 patients imaged with [^{68}Ga]Pentixafor-PET had biopsy-proven extramedullary relapse of AML after allogeneic stem cell transplantation (SCT) in the absence of BM involvement. [^{68}Ga]Pentixafor-PET/CT imaging in this patient revealed visually positive extramedullary disease and normal background BM signal. The extramedullary lesion showed a SUVmax of 5.2, comparable to the meanSUVmax measured in the BM of [^{68}Ga]Pentixafor-PET positive patients. Moreover, this CXCR4 positive lesion displayed high [^{18}F]FDG uptake (SUVmax 9.51) in the routine diagnostic [^{18}F]FDG-PET (*Online Supplementary Figure S4*).

To correlate *in vivo* imaging of CXCR4 with its expression level within the AML compartment, immunohistochemistry for CXCR4 was performed in 3 patients where BM biopsies in close time proximity to PET imaging were available. The high CXCR4 expression determined by IHC in Patient #1 and Patient #4 correlated well with tracer uptake detected by [^{68}Ga]Pentixafor-PET. Patient #10, who was visually negative in [^{68}Ga]Pentixafor-PET, revealed an undetectable to low CXCR4 expression as assessed by IHC (Figure 5).

In summary, these results reveal that *in vivo* imaging of myeloid malignancies, especially AML, is feasible with the new PET-tracer [^{68}Ga]Pentixafor. The variability in PET positivity for CXCR4 reflects the wide range of CXCR4 surface expression obtained with flow cytometry. Due to the limited number of patients, and the missing data on CXCR4 surface expression at the time of imaging in several patients, a statistically significant correlation between Pentixafor uptake and CXCR4 surface expression analyzed by flow cytometry and/or IHC cannot be made at this time; this will be investigated in a large planned prospective study (*EudraCT 2014-003411-12*).

Discussion

There are compelling data to show that the BM microenvironment contributes to treatment resistance and relapse in AML. CXCR4 and its ligand CXCL12 are essential for retention of normal HSPC and LICs within their protective niche and are, therefore, considered attractive targets for overcoming microenvironment-mediated resistance and inevitable subsequent clinical leukemia relapse.

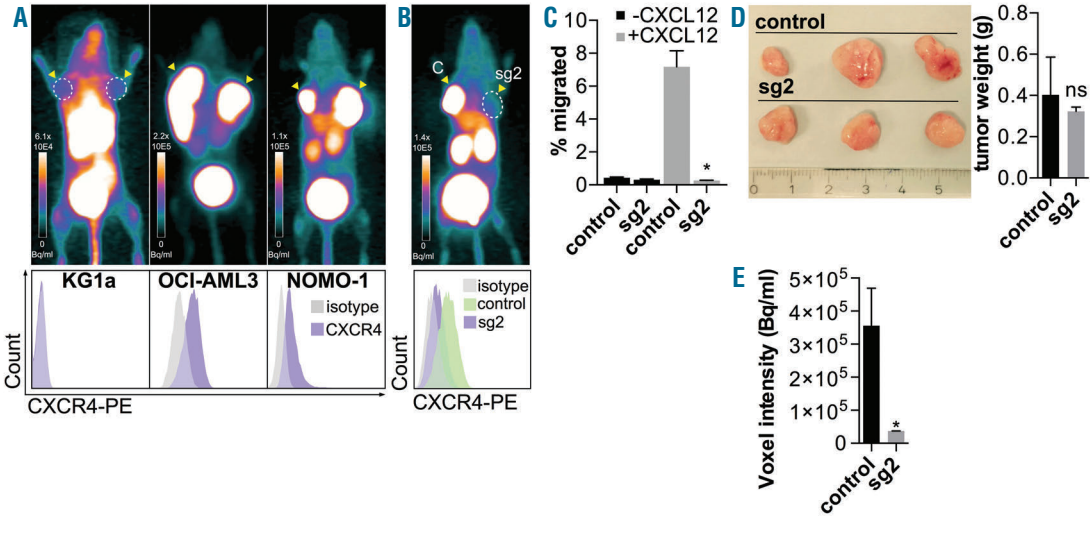

Figure 3. *In vivo* Pentixafor PET imaging in acute myeloid leukemia (AML) correlates with CXCR4 surface expression and migration towards a CXCL12 gradient. (A) [^{68}Ga]Pentixafor-PET imaging of AML xenografts. The indicated cell lines were injected into immunodeficient mice to generate xenograft tumors. CXCR4 expression was then analyzed using *in vivo* [^{68}Ga]Pentixafor-PET (upper panels). CXCR4 surface expression was analyzed by flow cytometry (lower panels). N=2 tumors/cell line; n=1 mouse/cell line. (B) [^{68}Ga]Pentixafor-PET imaging of control and CXCR4 knock-out (sg2) OCI-AML3 xenografts (upper panel). The lower panel shows CXCR4 surface expression as assessed by CD184 flow cytometry. A representative image and histogram is shown. (C) CRISPR/Cas9-mediated CXCR4 knock-out results in significantly reduced migration towards a CXCL12 gradient. OCI-AML3 cells were assessed using a transwell chamber migration assay. N=3 independent experiments. Mean±SEM is shown. *P=0.002 (Student's t-test). (D) Images of the explanted tumor shown in (B) and (C) (left panel). Tumor weight (right panel). Mean±SEM, no significant difference. (E) Quantification of [68Ga]Pentixafor uptake. Xenograft tumors were analyzed by means of voxel intensity measurement. Mean±SEM is shown, n=3 tumors for control and sg2, n=3 mice; *P=0.049 (Student's t-test).

The clinical significance of CXCR4 in AML is underscored by data showing that high CXCR4 expression on AML blasts correlates with poor prognosis.[17,37-39] In a pediatric AML cohort, blast CXCR4 surface expression was increased by chemotherapy and contributed to resistance.[40] There was no significant difference in CXCR4 surface expression between prognostic groups according to the modified ELN prognostic system[34] in our cohort, possibly due to sample size. In agreement with previous studies, CXCR4 surface expression in our cohort was highly variable. High CXCR4 expression correlated with high blast counts in our cohort, which might account for the poor prognosis seen in other studies. In addition to aberrant expression of CXCR4 in a substantial proportion of AML patients, ligand-mediated phosphorylation of serine 339 of CXCR4 appears to drive resistance to chemotherapy, and to increase retention of AML cells within the BM.[41] Such augmented interaction with the BM niche, in partic-

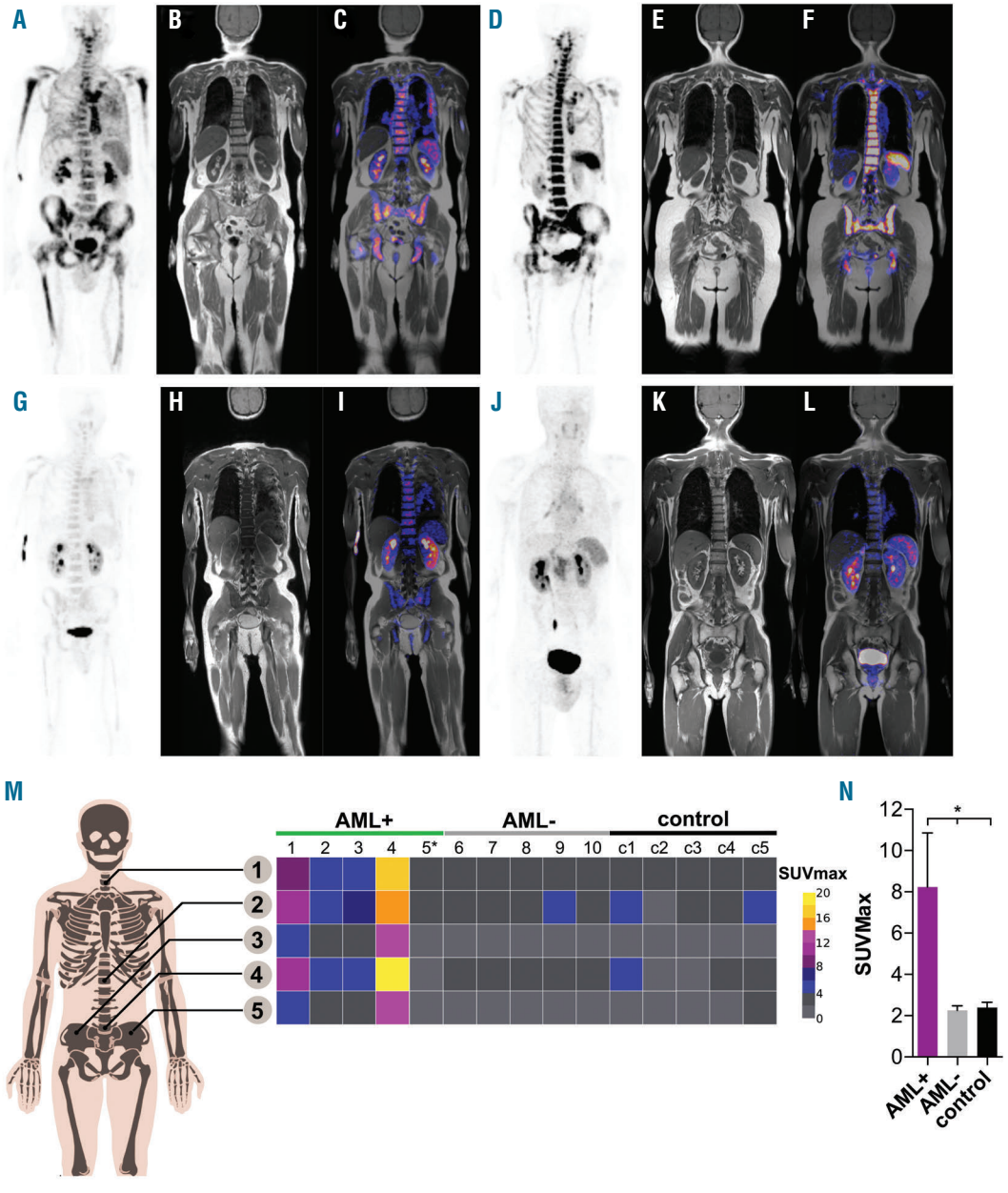

Figure 4. [^{68}Ga]Pentixafor-PET/magnetic resonance (MR) imaging in acute myeloid leukemia (AML) patients. (A-F) Shown are 2 AML patients (#2 and #1) with visually positive [^{68}Ga]Pentixafor-PET/MR imaging. (G-I)[^{68}Ga]Pentixafor-PET/MR images of a visually negative AML patient. (J-L) Control patient without BM malignancy who underwent [^{68}Ga]Pentixafor-PET/MR imaging. (A, D, G, J) Maximum intensity projections of [^{68}Ga]Pentixafor uptake. (B, E, H, K) T1w MR imaging coronal sections. (C, F, I, L) Coronal PET/MR imaging fusion. (M) (Left) Schematic graph of locations assessed for SUV quantification. 1: cervical vertebra (7); 2: thoracic vertebra (12); 3: right os ilium; 4: lumbal vertebra (5); 5: left os ilium. (Right) Heatmap of SUV values in the 5 visually positive (AML$^+$), 5 visually negative (AML$^-$), and 5 control patients with non-hematologic disease (control). *Patient #5 was scored positive because of a [^{68}Ga]Pentixafor-PET positive extramedullary lesion. (N) Quantification of SUV values from (m). *P=0.036 for AML$^+$ *versus* AML$^-$ and P=0.040 for AML$^+$ *versus* control. Error Bars represent the SEM. Patient #5 was excluded due to the lack of bone marrow involvement (extramedullary AML).

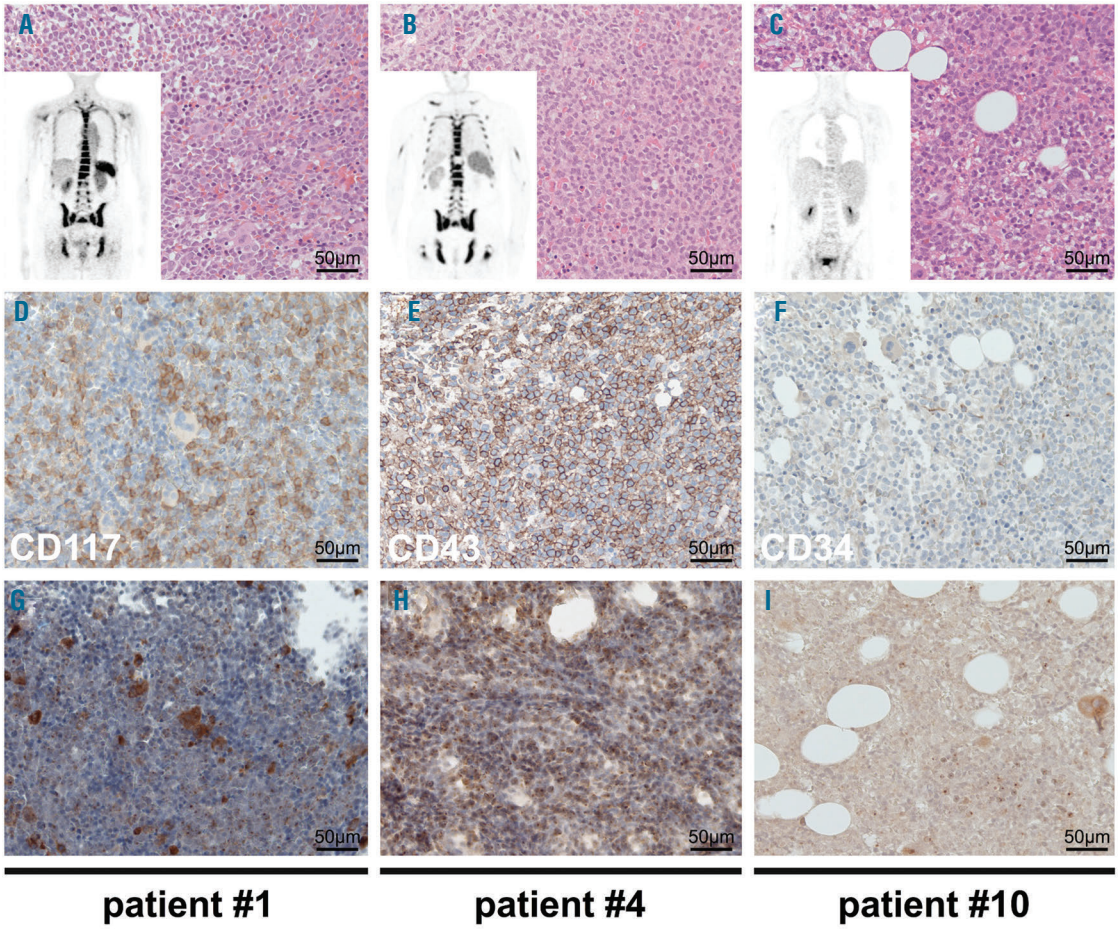

Figure 5. CXCR4 expression in bone marrow of acute myeloid leukemia (AML) patients undergoing [^{68}Ga]Pentixafor imaging. (A-C) Representative H&E stains of 3 AML patients show hypercellular bone marrow (BM) with blast infiltration; embedded are the PET images of the corresponding patients; (A) and (B) are visually positive for CXCR4-directed PET and (C) is negative. (D-F) IHC for patient specific myeloid/blast markers; stained markers are shown in white. (G-I) IHC for CXCR4 in the corresponding BM samples. (A, D, G) Patient #1. (B, E, H) Patient #4. (C, F, I) Patient #10.

ular differentiating osteoblasts, has recently been shown to counteract the induction of apoptosis within the leukemic compartment which can be triggered by CXCL12 ligation to CXCR4.[42,43] Against this background, it is currently unclear what impact CXCR4 targeting by small molecule CXCR4 antagonists or monoclonal antibodies will have in the clinic, and, in particular, on eliminating the LICs that fundamentally contribute to relapse. Despite this mechanistic uncertainty, the first-in-class CXCR4 inhibitor AMD3100 (Plerixafor) has been tested as a chemosensitizing agent in relapsed or refractory AML in a phase I/II trial with encouraging preliminary results.[44] Further trials involving monoclonal antibodies and novel CXCR4-targeting small molecule inhibitors such as BL-8040 are under way (*EudraCT 2014-002702-21*). Disrupting ligand-mediated CXCR4 downstream activity by antagonists is one approach currently being tested. Physically targeting the BM niche characterized by the CXCR4-CXCL12 interaction could be an attractive alternative. One highly interesting method that provides such physical targeting is peptide receptor radionuclide therapy (PRRT). PRRT has been successfully integrated into the therapeutic algorithm of neuroendocrine tumors (NETs).[45] It usually involves the diagnostic imaging of the receptor to ensure target expression, followed by the application of a therapeutically labeled peptide (e.g. Lutetium-177 octreotate), thus constituting a theranostic procedure. In patients with AML, an endoradiotherapeutic approach with CD45 as target has been successfully tested in a phase I/II trial in the conditioning regimen prior to allogeneic SCT.[46] For such a purpose, the data presented within our CXCR4 examinations represent an important step, as they show that, at least in a subgroup of patients, there is a substantial expression of CXCR4, and that AML can even be imaged using the novel CXCR4-specific molecular PET probe Pentixafor. Pentixafor has already been labeled with therapeutic radionuclides such as ^{99}Yttrium and 177Lutetium, and compassionate use therapies have been applied to patients with very advanced multiple myeloma.[25] A phase I/II study in myeloma using the CXCR4-directed theranostic approach is currently under investigation (*EudraCT 2015-001817-28*). With regard to AML, however, it is still not at all clear whether measurable high CXCR4 expression is a prerequisite for such a therapy, since it can be assumed that targeting the niche *via* CXCR4 could have an effect on all hematopoietic cells harbored there. The imaging data presented in our study reveals crucial information on *in vivo* CXCR4 expression in

myeloid malignancy. Although we still have no data on ALL, very recent work defines the CXCR4/CXCL12 interaction as crucial for disease maintenance and progression in ALL.[18,19]

We are continuing to learn more about both the molecular and the genetic characterization of AML and ALL.[47] Thus, markers for detecting MRD are available that provide high sensitivity,[48] avoiding the need for additional imaging. We foresee the major application of CXCR4 targeting using the herein described CXCR4-binding peptide within a theranostic approach, i.e. as a conditioning regimen within an allogeneic SCT. The importance of the CXCR4/CXCL12 axis as a label of the LIC niche, as well as the observation that relapsed leukemias frequently express high levels of CXCR4, makes radiolabeled CXCR4 targeting an attractive novel therapeutic approach.

Acknowledgments

The authors would like to thank the staff of the diagnostic laboratory of the III Medical Department and the staff of the small animal PET facility of the Nuclear Medicine Department, TU München, Germany, for their assistance.

Funding

UK, HJW, and MS received support from the Deutsche Forschungsgemeinschaft (DFG, SFB824). UK was further supported by DFG (grant KE 222/7-1). This work received support from the German Cancer Consortium (DKTK).

References

1. Byrd JC, Mrozek K, Dodge RK, et al. Pretreatment cytogenetic abnormalities are predictive of induction success, cumulative incidence of relapse, and overall survival in adult patients with de novo acute myeloid leukemia: results from Cancer and Leukemia Group B (CALGB 8461). Blood. 2002;100(13):4325-4336.
2. Mayer RJ, Davis RB, Schiffer CA, et al. Intensive postremission chemotherapy in adults with acute myeloid leukemia. Cancer and Leukemia Group B. N Engl J Med. 1994;331(14):896-903.
3. Sekeres MA. Treatment of older adults with acute myeloid leukemia: state of the art and current perspectives. Haematologica. 2008;93(12):1769-1772.
4. Schepers K, Campbell TB, Passegue E. Normal and leukemic stem cell niches: insights and therapeutic opportunities. Cell Stem Cell. 2015;16(3):254-267.
5. Sipkins DA, Wei X, Wu JW, et al. In vivo imaging of specialized bone marrow endothelial microdomains for tumour engraftment. Nature. 2005;435(7044):969-973.
6. Matsunaga T, Takemoto N, Sato T, et al. Interaction between leukemic-cell VLA-4 and stromal fibronectin is a decisive factor for minimal residual disease of acute myelogenous leukemia. Nat Med. 2003;9(9):1158-1165.
7. Sugiyama T, Kohara H, Noda M, Nagasawa T. Maintenance of the hematopoietic stem cell pool by CXCL12-CXCR4 chemokine signaling in bone marrow stromal cell niches. Immunity. 2006;25(6):977-988.
8. Shen H, Cheng T, Olszak I, et al. CXCR-4 desensitization is associated with tissue localization of hemopoietic progenitor cells. J Immunol. 2001;166(8):5027-5033.
9. Peled A, Petit I, Kollet O, et al. Dependence of human stem cell engraftment and repopulation of NOD/SCID mice on CXCR4. Science. 1999;283(5403):845-848.
10. Lapidot T. Mechanism of human stem cell migration and repopulation of NOD/SCID and B2mnull NOD/SCID mice. The role of SDF-1/CXCR4 interactions. Ann N Y Acad Sci. 2001;938:83-95.
11. Zou YR, Kottmann AH, Kuroda M, Taniuchi I, Littman DR. Function of the chemokine receptor CXCR4 in haematopoiesis and in cerebellar development. Nature. 1998;393(6685):595-599.
12. Zhao H, Guo L, Zhao H, et al. CXCR4 overexpression and survival in cancer: a system review and meta-analysis. Oncotarget. 2015;6(7):5022-5040.
13. Teicher BA, Fricker SP. CXCL12 (SDF-1)/CXCR4 pathway in cancer. Clin Cancer Res. 2010;16(11):2927-2931.
14. Tavor S, Petit I, Porozov S, et al. CXCR4 regulates migration and development of human acute myelogenous leukemia stem cells in transplanted NOD/SCID mice. Cancer Res. 2004;64(8):2817-2824.
15. Lapidot T, Sirard C, Vormoor J, et al. A cell initiating human acute myeloid leukaemia after transplantation into SCID mice. Nature. 1994;367(6464):645-648.
16. Kollet O, Spiegel A, Peled A, et al. Rapid and efficient homing of human CD34(+)CD38(-/low)CXCR4(+) stem and progenitor cells to the bone marrow and spleen of NOD/SCID and NOD/SCID/B2m(null) mice. Blood. 2001;97(10):3283-3291.
17. Spoo AC, Lubbert M, Wierda WG, Burger JA. CXCR4 is a prognostic marker in acute myelogenous leukemia. Blood. 2007;109(2):786-791.
18. Pitt LA, Tikhonova AN, Hu H, et al. CXCL12-Producing Vascular Endothelial Niches Control Acute T Cell Leukemia Maintenance. Cancer Cell. 2015;27(6):755-768.
19. Passaro D, Irigoyen M, Catherinet C, et al. CXCR4 Is Required for Leukemia-Initiating Cell Activity in T Cell Acute Lymphoblastic Leukemia. Cancer Cell. 2015;27(6):769-779.
20. Cho B-S, Zeng Z, Mu H, et al. Antileukemia activity of the novel peptidic CXCR4 antagonist LY2510924 as monotherapy and in combination with chemotherapy. Blood. 2015;126(2):222-232.
21. Zeng Z, Shi YX, Samudio IJ, et al. Targeting the leukemia microenvironment by CXCR4 inhibition overcomes resistance to kinase inhibitors and chemotherapy in AML. Blood. 2009;113(24):6215-6224.
22. Nervi B, Ramirez P, Rettig MP, et al. Chemosensitization of acute myeloid leukemia (AML) following mobilization by the CXCR4 antagonist AMD3100. Blood. 2009;113(24):6206-6214.
23. Philipp-Abbrederis K, Herrmann K, Knop S, et al. In vivo molecular imaging of chemokine receptor CXCR4 expression in patients with advanced multiple myeloma. EMBO Mol Med. 2015;7(4):477-487.
24. Wester HJ, Keller U, Schottelius M, et al. Disclosing the CXCR4 expression in lymphoproliferative diseases by targeted molecular imaging. Theranostics. 2015;5(6):618-630.
25. Herrmann K, Schottelius M, Lapa C, et al. First-in-man experience of CXCR4-directed endoradiotherapy with 177Lu- and 90Y-labelled pentixather in advanced stage multiple myeloma with extensive intra- and extramedullary disease. J Nucl Med. 2016;57(2):248-251.
26. Haug AR, Cindea-Drimus R, Auernhammer CJ, et al. Neuroendocrine tumor recurrence: diagnosis with 68Ga-DOTATATE PET/CT. Radiology. 2014;270(2):517-525.
27. Brinkman EK, Chen T, Amendola M, van Steensel B. Easy quantitative assessment of genome editing by sequence trace decomposition. Nucleic Acids Res. 2014;42(22):e168.
28. Demmer O, Gourni E, Schumacher U, Kessler H, Wester HJ. PET Imaging of CXCR4 receptors in cancer by a new optimized ligand. Chem Med Chem. 2011;6(10):1789-1791.
29. Gourni E, Demmer O, Schottelius M, et al. PET of CXCR4 expression by a (68)Ga-labeled highly specific targeted contrast agent. J Nucl Med. 2011;52(11):1803-1810.
30. Martin R, Juttler S, Muller M, Wester HJ. Cationic eluate pretreatment for automated synthesis of [(6)(8)Ga]CPCR4.2. Nucl Med Biol. 2014;41(1):84-89.
31. Drzezga A, Souvatzoglou M, Eiber M, et al. First clinical experience with integrated whole-body PET/MR: comparison to PET/CT in patients with oncologic diagnoses. J Nucl Med. 2012;53(6):845-855.
32. Silva JR Jr, Hayashi D, Yonenaga T, et al. MRI of bone marrow abnormalities in hematological malignancies. Diagn Interv Radiol. 2013;19(5):393-399.
33. Zamagni E, Patriarca F, Nanni C, et al. Prognostic relevance of 18-F FDG PET/CT in newly diagnosed multiple myeloma patients treated with up-front autologous transplantation. Blood. 2011;118(23):5989-5995.
34. Estey EH. Acute myeloid leukemia: 2014 update on risk-stratification and management. Am J Hematol. 2014;89(11):1063-1081.
35. Sanjana NE, Shalem O, Zhang F. Improved vectors and genome-wide libraries for

CRISPR screening. Nat Methods. 2014;11 (8):783-784.
36. De Silva RA, Peyre K, Pullambhatla M, et al. Imaging CXCR4 Expression in Human Cancer Xenografts: Evaluation of Monocyclam Cu-64-AMD3465. J Nucl Med. 2011;52(6):986-993.
37. Rombouts EJ, Pavic B, Lowenberg B, Ploemacher RE. Relation between CXCR-4 expression, Flt3 mutations, and unfavorable prognosis of adult acute myeloid leukemia. Blood. 2004;104(2):550-557.
38. Tavernier-Tardy E, Cornillon J, Campos L, et al. Prognostic value of CXCR4 and FAK expression in acute myelogenous leukemia. Leuk Res. 2009;33(6):764-768.
39. Bae MH, Oh SH, Park CJ, et al. VLA-4 and CXCR4 expression levels show contrasting prognostic impact (favorable and unfavorable, respectively) in acute myeloid leukemia. Ann Hematol. 2015;94(10):1631-1638.
40. Sison EA, McIntyre E, Magoon D, Brown P. Dynamic chemotherapy-induced upregulation of CXCR4 expression: a mechanism of therapeutic resistance in pediatric AML. Mol Cancer Res. 2013;11(9):1004-1016.
41. Brault L, Rovo A, Decker S, et al. CXCR4-SERINE339 regulates cellular adhesion, retention and mobilization, and is a marker for poor prognosis in acute myeloid leukemia. Leukemia. 2014;28(3):566-576.
42. Kremer KN, Dudakovic A, McGee-Lawrence ME, et al. Osteoblasts protect AML cells from SDF-1-induced apoptosis. J Cell Biochem. 2014;115(6):1128-1137.
43. Kremer KN, Peterson KL, Schneider PA, et al. CXCR4 chemokine receptor signaling induces apoptosis in acute myeloid leukemia cells via regulation of the Bcl-2 family members Bcl-XL, Noxa, and Bak. J Biol Chem. 2013;288(32):22899-22914.
44. Uy GL, Rettig MP, Motabi IH, et al. A phase 1/2 study of chemosensitization with the CXCR4 antagonist plerixafor in relapsed or refractory acute myeloid leukemia. Blood. 2012;119(17):3917-3924.
45. van Essen M, Krenning EP, Bakker WH, et al. Peptide receptor radionuclide therapy with 177Lu-octreotate in patients with foregut carcinoid tumours of bronchial, gastric and thymic origin. Eur J Nucl Med Mol Imaging. 2007;34(8):1219-1227.
46. Pagel JM, Gooley TA, Rajendran J, et al. Allogeneic hematopoietic cell transplantation after conditioning with 131I-anti-CD45 antibody plus fludarabine and low-dose total body irradiation for elderly patients with advanced acute myeloid leukemia or high-risk myelodysplastic syndrome. Blood. 2009;114(27):5444-5453.
47. Swerdlow SH, Campo E, Harris NL, et al. WHO Classification of Tumours of Haematopoietic and Lymphoid Tissues. IARC. 2008.
48. Ossenkoppele GJ, Schuurhuis GJ. MRD in AML: it is time to change the definition of remission. Best Pract Res Clin Haematol. 2014;27(3-4):265-271.